Iron and Ruthenium Glycoporphyrins: Active Catalysts for the Synthesis of Cyclopropanes and Aziridines

Caterina Damiano, Sebastiano Gadolini, Daniela Intrieri, Luigi Lay*, Cinzia Colombo and Emma Gallo*

Abstract: In view of the relevance of cyclopropanes and aziridines as synthetic building blocks as well as active parts in biological and pharmaceutical compounds, the development of sustainable synthetic procedures for obtaining these products continues to be a significant challenge. Herein, we report the synthesis of iron and ruthenium glycoporphyrins and their catalytic activity in promoting cyclopropanations and aziridinations by using diazo compounds and aryl azides as carbene and nitrene precursors, respectively. The number and location of carbohydrate units on the porphyrin skeleton modulated the shape- and diasteroselectivity of the reactions. Interestingly, while iron(III) glycoporphyrins showed good performances in alkene cyclopropanations, ruthenium(II) complexes performed better in aziridination reactions. Although none of the reported complexes induced enantiocontrol, probably due to the long distance between the chiral carbohydrate and the active metal centre, excellent *trans*-diasteroselectivities were observed by using iron-glycoporphyrins as cyclopropanation promoters.

Introduction

Three-membered ring compounds, such as cyclopropanes and aziridines, are valuable molecules due to their high chemical reactivity and their presence in the organic skeleton of biological and pharmaceutical products.[1] Thus, a large interest has been focused on the development of efficient synthetic procedures to obtain these classes of compounds. The direct reaction of alkenes with carbene [$C(R^2)R^3$] and nitrene [NAr] precursors, such as diazo compounds and aryl azides respectively, are atom-efficient strategies due to the formation of the eco-friendly N_2 as the only stoichiometric by-product (Scheme 1).[2]

C. Damiano, S. Gadolini, PhD D. Intrieri, Prof. L. Lay* PhD C. Colombo and Prof. E. Gallo*
Department of Chemistry, University of Milan, Via Golgi 19
E-mail: emma.gallo@unimi.it; luigi.lay@unimi.it

Supporting information for this article is given via a link at the end of the document.

Scheme 1. Reaction of styrenes with either diazo compounds (*path a*) or aryl azides (*path b*).

Among transition metal complexes, which have been used for mediating these transformations,[3] metal porphyrins represent a very powerful class of molecules,[4] whose properties can be modulated by introducing suitable substituents onto the skeleton. Carbohydrates are interesting bio-scaffold molecules for the porphyrin functionalisation, since their features can be exploited for varying the chemical nature of porphyrin ligands and in turn, the chemo-physical properties of the catalysts. Although glycoporphyrins have largely been described for biological and pharmaceutical applications,[5] their use as ligands in catalysis has been still limited.[6]

Some years ago, we reported the synthesis and catalytic activity of different metal glycoporphyrins, which were very efficient in promoting benzylic C-H bond aminations by organic azides.[7] These promising results prompted us to also study the catalytic activity of metal glycoporphyrins in cyclopropanations and aziridinations of alkenes. The dependence of catalytic performances on the number and location of carbohydrate units on the porphyrin skeleton is here reported.

Results and Discussion

Considering that the molecular structure of the porphyrin ring plays an important role in determining the efficiency of the corresponding metal catalysts, *mono* and *tetra* glycosyl-substituted porphyrins were synthesised to assess how the number and location of carbohydrate units can influence the catalytic activity of their relative ruthenium and iron complexes. First, porphyrins **2** and **3**, showing one or four carbohydrate units on the *para* position of the *meso*-aryl group, were obtained by using minor modifications of a methodology already reported by us.[7]

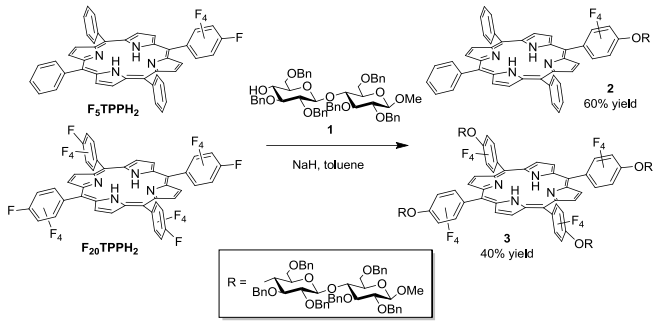

Scheme 2. Synthesis of *mono* and *tetra* glycoporphyins **2** and **3**.

The direct reaction of cellobioside **1**[8] with either **F_5TPPH_2**[9] or **$F_{20}TPPH_2$**[10] porphyrin afforded glycoporphyrins **2** and **3** in 60% and 40% yields, respectively (Scheme 2). From a synthetic point of view, the presence of one or four C_6F_5 *meso* substituents allowed the anchoring of the desired number (one or four) of carbohydrate units onto the porphyrin skeleton by a nucleophilic substitution of the *para* fluorine atom of the C_6F_5 moiety.

On the other hand, the C_2-symmetrical tetra-carbohydrate porphyrin **7** was obtained by following the procedure reported in Scheme 3. Porphyrin **4**[11] was used as the starting material to take advantage of its pre-organised symmetry, which plays an important role in determining the reaction diasteroselectivity (this aspect will be further discussed in the catalytic section).

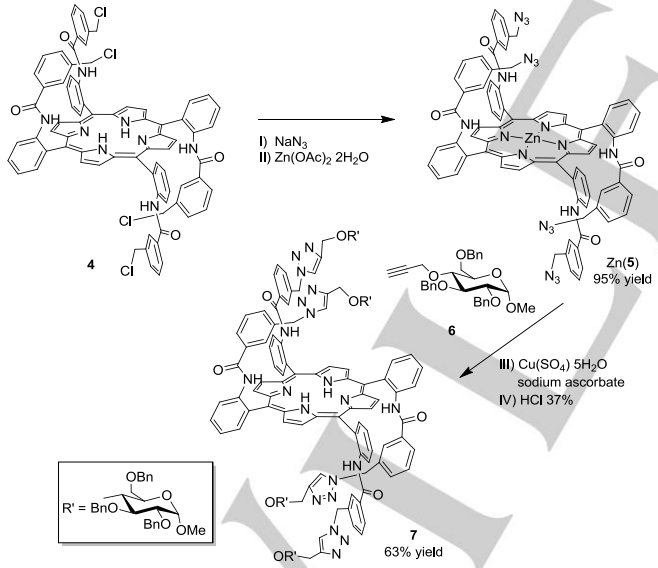

Scheme 3. Synthesis of C_2-symmetrical porphyrin **7**.

The reaction of benzyl chloride pickets of porphyrin **4** with NaN_3 forms, in 95% yield, the corresponding azido derivative **5,** which yields Zn(**5**) in a quantitative yield by reacting with $Zn(OAc)_2$ $2H_2O$. Then, the "click" reaction of Zn(**5**) with glucoside **6**,[12] which was prepared by reacting the corresponding methyl 2,3,6-tri-*O*-benzyl-α-D-glucopyranoside with propargyl bromide in the presence of sodium hydride, yielded Zn(**7**). Finally, the free base porphyrin **7** was obtained by removing the Zn atom with HCl 37%. Although the synthetic procedure to obtain **7** requires four steps, three of them occurred in quantitative yields and one with a yield up to 63%. The synthesis of **7** was performed at low temperatures (under 50°C) to avoid the formation of the statistical distribution of atropoisomers.[11, 13]

The so-obtained porphyrins **2**, **3** and **7**, as well as their precursors **F_5TPPH_2** and **$F_{20}TPPH_2$**, were employed to synthesise corresponding iron and ruthenium complexes (Figure 1) to be tested as catalysts of cyclopropanation and aziridination reactions. Importantly, the catalytic activity of iron and ruthenium derivatives of **F_5TPPH_2** and **$F_{20}TPPH_2$** porphyrins was investigated to better evaluate the influence of carbohydrates on the catalytic performances.

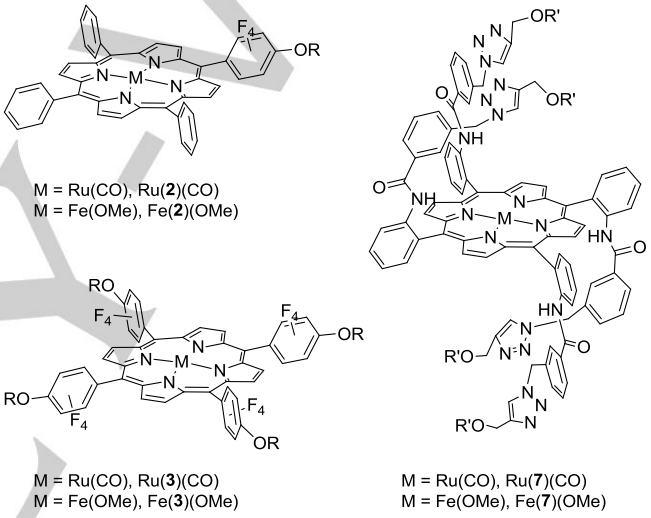

Figure 1. Ruthenium and iron glycosylated porphyrin complexes.

All Fe(porphyrin)OMe complexes were easily obtained by refluxing the desired porphyrin ligand with an excess of $FeBr_2$ in anhydrous THF for 5 hours. As previously reported,[14] the oxidation of the initially formed Fe(II) species by atmospheric oxygen was responsible for the formation of Fe(III) complexes. The anchorage of the methoxy axial ligand to the metal occurred both during the MeOH-based chromatography purification and the final treatment of the complexes with MeOH at 50°C. All synthesised Fe(porphyrin)OMe complexes were characterised by elemental analysis, UV/VIS and MS spectroscopy (see experimental section).

The insertion of ruthenium into porphyrin rings generally requires experimental conditions more drastic than those employed for the iron insertion. Indeed, Ru(**F_5TPP**)CO, Ru(**$F_{20}TPP$**)CO and Ru(**2**)CO were obtained by refluxing the corresponding ligand with an excess of $Ru_3(CO)_{12}$ in 1,2,3-trichlorobenzene as the reaction solvent. Considering that Ru(**3**)CO was not obtained by simply treating $Ru_3(CO)_{12}$ with ligand **3**, an alternative strategy was applied. Complex Ru(**$F_{20}TPP$**)CO was first synthesised and then reacted with **1** in the presence of sodium hydride to yield

Ru(**3**)CO in 39% yield. Unfortunately, all the above described procedures failed for the insertion of ruthenium into porphyrin **7**. Thus, Ru(**7**)CO complex was obtained in 19% yield by reacting porphyrin **7** with $Ru_3(CO)_{12}$ in a pressure tube at 150°C, using toluene as the reaction solvent. The low yield in which Ru(**7**)CO was obtained can be due to the high working temperature (150°C) which, by promoting the ligand atropoisomerization, may be responsible for the formation of the desired ruthenium complex in a limited amount.

The activity of all the synthesised iron and ruthenium complexes was initially tested in the model cyclopropanation reaction between α–methylstyrene and ethyl diazoacetate (EDA) forming **8**, and the achieved results are shown in Table 1.

Table 1. Synthesis of **8** catalysed by iron(III) and ruthenium(II) glycoporphyrin complexes.[a]

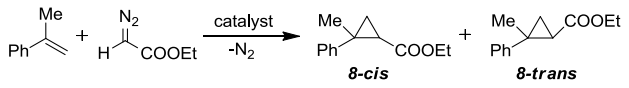

entry	catalyst	yield (%)[b]	*trans/cis*[b]
1	Fe(**F$_5$TPP**)(OMe)	80	87:13
2	Fe(**2**)(OMe)	80	88:12
3	Ru(**F$_5$TPP**)(CO)	70	88:12
4	Ru(**2**)(CO)	68	90:10
5	Fe(**F$_{20}$TPP**)(OMe)	60	60:40
6	Fe(**3**)(OMe)	71	80:20
7	Ru(**F$_{20}$TPP**)(CO)	45	60:40
8	Ru(**3**)(CO)	61	78:22
9	Fe(**7**)(OMe)	69	95:5
10	Ru(**7**)(CO)	66	95:5

[a] Reactions were stirred in toluene for 2 h at 25°C by using catalyst/EDA/α-methylstyrene = 1:1100:5000. [b] Determined by ^{1}H NMR spectroscopy using 2,4-dinitrotoluene as the internal standard.

The conjugation of **F$_5$TPPH$_2$** with one saccaride unit (**1**) forming porphyrin **2** was not responsible for an enhancement of the catalytic performances of corresponding iron and ruthenium derivatives. In fact, analogous results, both in terms of yields and diastereoselectivities, were obtained (compare entries 1 and 3 with 2 and 4, Table 1). On the other hand, both Fe(**3**)(OMe) and Ru(**3**)(CO) were more productive than their parent Fe(**F$_{20}$TPP**)(OMe) and Ru(**F$_{20}$TPP**)CO compounds to indicate a positive effect of the insertion of four carbohydrate units onto the porphyrin skeleton. A better diastereocontrol was also observed (compare entries 5 and 7 with 6 and 8, Table 1). Finally, even if cyclopropanes **8** (*cis* + *trans*) were obtained with lower yields by using Fe(**7**)(OMe) and Ru(**7**)(CO), these two catalysts were responsible for the best reaction diastereoselectivities (Table 1, entries 9 and 10).

Note that porphyrins **3** and **7** contain the same number of carbohydrate units, which are respectively located in *para* position of the *meso* aromatic moiety in ligand **3** and on the pickets of the C_2 symmetrical skeleton of **7**. While the different location of the four carbohydrate units did not influence the reaction yields, the position of the carbohydrate moiety had a relevant effect on the reaction diastereoselectivity. In accordance with our previous studies,[14b] the C_2-symmetry of the porphyrinic skeleton of **7** was responsible for the highest diastereocontrol, independently of the nature of the active metal (compare entries 9 and 10 with entries 6 and 8, Table 1). It is important to point out that, while the nature of the final chiral pickets was not crucial for determining the *trans*-diastereoselectivity, their electronic and steric features were responsible for the enantioselective induction.[14] In fact, even though similar diastereoselectivities were observed in the presence of a porphyrin catalyst obtained by functionalizing the $\alpha_2\beta_2$ parent porphyrin **4** (Scheme 3) with either binaphthyl[14b] or amino acid chiral units,[14c] the reaction enantioselectivity was very different in the two cases.

Unfortunately, none of the complexes reported in Table 1 induced an enantiocontrol, probably due to the long distance between the chiral carbohydrates and the active metal centre.

Although the efficiency of glycoporphyrin complexes was comparable to those of their precursors, the catalytic activity of glycoporphyrin complexes has been further investigated in view of the excellent diastero discriminations achieved a high potential of these catalytic systems.

In fact, the presence of saccharides in the ligand skeleton will be exploited to perform catalytic reactions in a biphasic medium, after deprotection of the carbohydrate moieties.

Complex Fe(**2**)OMe was selected as the most convenient catalyst to study the reaction scope in view of i) the catalytic results of Table 1, ii) the importance of using eco-compatible non-noble metal catalysts and iii) the easier synthetic accessibility of porphyrin **2** with respect to ligands **3** and **7**, which facilitates to obtain corresponding metal catalysts in significant amounts for affordable applications of the methodology. Obtained results are reported in Table 2.

Catalytic tests were performed by using either the molar ratio Fe(**2**)OMe/EDA/alkene = 1:1100:5000, or a slight EDA excess with respect to the alkene substrate (Fe(**2**)OMe/EDA/alkene = 1:1100:1000). Reported data indicated that an alkene excess was necessary for suppressing the EDA homo-coupling process, which in turn decreases the cyclopropane yields. The catalytic productivity was influenced by the steric hindrance of the aromatic portion of the employed alkene, as proven by the lower yield that was observed by using 2-methylstyrene instead of 3-methylstyrene or 4-methylstyrene, as the reaction substrate (products **10**, **11** and **12**). The best yields were achieved by using *para*-substituted α-methylstyrene, independently of the electronic nature of the alkene substituent (products **8**, **14** and **15**). Very good *trans*-diastereoselectivities, up to 92:8, were obtained for all the tested catalytic reactions.

Table 2. Synthesis of cyclopropanes **8**-**15** catalysed by Fe(**2**)(OMe).[a]

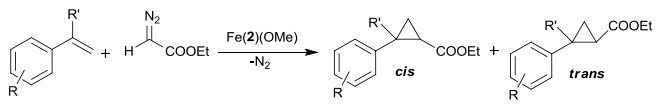

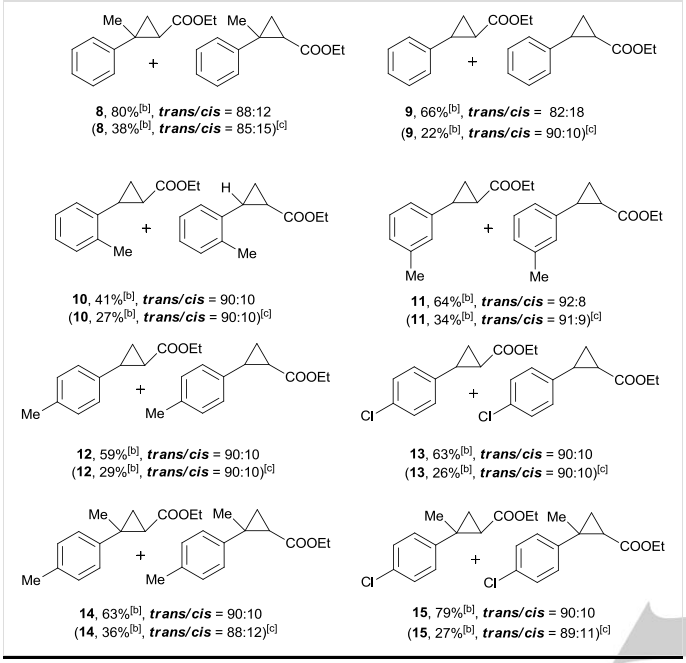

[a] Reactions were stirred in toluene for 2 h at 25°C by using Fe(**2**)(OMe)/EDA/alkene = 1:1100:5000. [b] Determined by ^{1}H NMR spectroscopy using 2,4-dinitrotoluene as the internal standard. [c] Fe(**2**)(OMe)/EDA/alkene = 1:1100:1000.

Next, styrene and α-methylstyrene were reacted, in the presence of Fe(**2**)OMe, with diazo derivatives showing different steric hindrances and electronic features by using experimental conditions reported in Table 2. While the only-acceptor (COOtBu)CHN$_2$ compound reacted with styrene affording the corresponding cyclopropane **16** in 48% yield and a *trans*/*cis* ratio of 88:12 (see SI), the analogous reaction with the more sterically encumbered α-methylstyrene did not yield the desired cyclopropane. Unfortunately, the reaction of acceptor-acceptor and donor-acceptor substituted diazo compounds with either styrene or α-methylstyrene did not occur (Scheme 4).

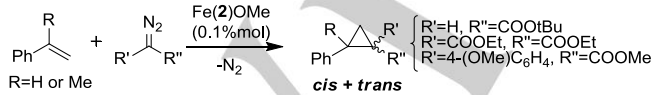

Scheme 4. Reactivity of diazo reagents in the Fe(**2**)OMe-catalysed cyclopropanation of styrene (R = H) and α-methylstyrene (R = Me).

Then, the catalytic activity of iron and ruthenium glycoporphyrin complexes as well as their precursors, was tested in the aziridination of α-methylstyrene by 3,5-*bis*(trifluoromethyl)phenyl azide, forming **17**. No aziridine was formed by using Fe(**F$_5$TPP**)(OMe), Fe(**2**)(OMe), Fe(**3**)(OMe) and Fe(**7**)(OMe) while, Fe(**F$_{20}$TPP**)(OMe) led to the formation of **17** in 90% yield. This result was in accordance with literature, which reports good activities for the **F$_{20}$TPP**-containing iron catalysts.[15]

Table 3. Synthesis of **17** catalysed by ruthenium complexes.[a]

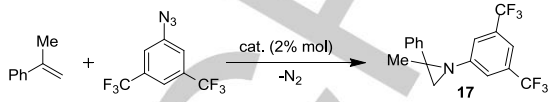

entry	catalyst	yield (%)[b]
1	Ru(**F$_5$TPP**)(CO)	81
2	Ru(**F$_{20}$TPP**)(CO)	83
3	Ru(**2**)CO	80
4	Ru(**3**)CO	17
5	Ru(**7**)CO	-

[a] Reactions were refluxed for 2 h in benzene by using catalyst/azide/α-methylstyrene = 1:50:250. [b] Determined by ^{1}H NMR spectroscopy using 2,4-dinitrotoluene as the internal standard.

On the other hand, while Ru(**3**)CO complex showed a limited catalytic efficiency (Table 3, entry 4), Ru(**F$_5$TPP**)(CO), Ru(**F$_{20}$TPP**)(CO) and Ru(**2**)CO mediated the synthesis of **17** in analogous yields (Table 3, entries 1, 2 and 3). Finally, Ru(**7**)CO was inactive in promoting the model reaction forming **17** (Table 3, entry 5) probably due to the tridimensional arrangement of the ligand, which hampered a productive interaction of substrates with the active ruthenium metal centre.

Considering what stated above on the prospective employment of glycoporphyrin catalysts and the good result that was obtained by performing the synthesis of **17** in the presence of Ru(**2**)CO, this complex was used to study the reactivity of α-methylstyrene towards different aryl azides. Achieved results are reported in Table 4.

Table 4. Synthesis of aziridines catalysed by Ru(**2**)(CO).[a]

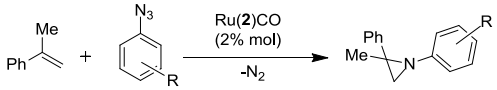

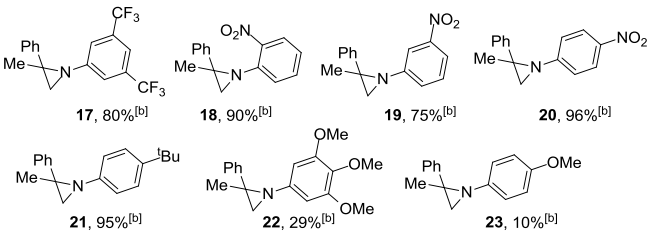

[a] Reactions were refluxed in benzene for 2 h by using Ru(**2**)(CO)/azide/α-methylstyrene = 1:50:250. [b] Determined by ^{1}H NMR spectroscopy using 2,4-dinitrotoluene as the internal standard.

Collected data indicate that the electronic nature of the aromatic azide seems not to strongly influence the Ru(**2**)CO catalytic performance. Indeed, comparable yields were obtained by using either 4-$(NO_2)C_6H_4N_3$ (Table 4, compound **20**) or 4-(^{t}Bu)$C_6H_4N_3$ (Table 4, compound **21**) azide. Very good aziridine yields were also observed by employing both *ortho* and *meta*-substituted (with respect the N_3 functionality) azides to indicate that the aziridine formation was slightly hampered by the presence of substituents close the reactive N_3 grouping (Table 4, compounds **17**, **18** and **19**).

Low yields were obtained by using azides bearing on the aryl moiety a coordinating substituent such as a methoxy group (Table 4, compounds **22** and **23**), which can be responsible for a catalytic deactivation by competing with the organic substrate for the metal centre. In accordance with that already reported by some of us,[16] the negative effect was more pronounced reacting α-methystyrene with 4-$(MeO)C_6H_4N_3$ than 3,4,5-$(MeO)_3C_6H_2N_3$ due to the better coordinating capability of an unhindered methoxy group compared to three contiguous ones (compare yields of products **22** and **23**).

Conclusions

In conclusion, we reported the synthesis and catalytic activity of three different iron and ruthenium glycoporphyrins and their related precursors. While iron(III) derivatives showed good performances in alkene cyclopropanations, ruthenium(II) complexes were efficient promoters of aziridination reactions. Among all synthesised catalysts, the catalytic activity of Fe(**2**)(OMe) and Ru(**2**)CO was further investigated because porphyrin **2** can be considered a valuable ligand being easily synthesised in good yields and the amphiphilic nature of **2** can be well suitable, after deprotection of the carbohydrate residue, to perform catalysis in a biphasic medium due to the presence of the hydrophilic carbohydrate and the lipophilic tetrapyrrolic core. In addition, the present work can pave the way to other investigations because the synthesis of **2** can be applied to anchor a polysaccharides to **F_5TPPH$_2$**. This synthetic strategy could be useful to incorporate low-toxic metal catalyst (e.g. iron derivatives) into a biologic scaffold in order to provide sustainable catalysts to be tested for eco-compatible catalytic applications in an aqueous medium.

Experimental Section

General Conditions. All catalytic reactions and some of the synthetic procedures reported (where specified) were carried out under nitrogen atmosphere employing standard Schlenk techniques and vacuum-line manipulations. All the solvents were dried by using standard procedures unless otherwise specified.

Reagents. Organic azides,[17] diazo compounds,[18] *meso*-tetrakis(pentafluorophenyl)porphyrin (**F_{20}TPPH$_2$**),[10] 5-(pentafluorophenyl)-10,15,20-triphenylporphyrin (**F_5TPPH$_2$**),[9] methyl 2,3,6-tri-O-benzyl-4-O-(2,3,6-tri-O-benzyl-β-D-glucopyranosyl)-β-D-glucopyranoside (**1**),[8] α-5,10-β-15,20-tetrakis(2-[(3-chloromethyl)benzoylamido]phenyl) porphyrin (**5**),[11] methyl 2,3,6-tri-O-benzyl-4-O-(prop-2-ynyl)- α-D-glucopyranoside (**6**),[12] **Ru(F_{20}TPP)(CO)**[19] were synthesised as reported in literature. Other starting materials have been purchased and used as received.

Instruments. NMR spectra were recorded at room temperature either on a Bruker Avance 300-DRX, operating at 300 MHz for ^{1}H, at 75 MHz for ^{13}C and at 282 MHz for ^{19}F, or on a Bruker Avance 400-DRX spectrometers, operating at 400 MHz for ^{1}H, 100 MHz for ^{13}C and 376 MHz for ^{19}F. Chemical shifts (ppm) are reported relative to TMS. The ^{1}H NMR signals of the compounds described in the following were attributed by 2D NMR techniques. Assignments of the resonance in ^{13}C NMR were made by using the APT pulse sequence, HSQC and HMBC techniques. Infrared spectra were recorded on a Varian Scimitar FTS 1000 spectrophotometer. UV/Vis spectra were recorded on an Agilent 8453E instrument. MALDI-TOF spectra were acquired either on a Bruker Daltonics Microflex or on a Bruker Daltonics Autoflex III TOF/TOF at C.I.G.A, University of Milan. High resolution MS (HR-MS) spectra were obtained on a Bruker Daltonics ICR-FTMS APEX II at C.I.G.A, University of Milan. Microanalysis was performed on a Perkin Elmer 2400 CHN Elemental Analyzer instrument.

Synthesis of 2. NaH 60% (128.0 mg, 5.32 mmol) was added under nitrogen to a toluene (28.0 mL) solution of **F_5TPPH$_2$** (150.0 mg, 2.13 x 10^{-1} mmol) and **1** (380.0 mg, 4.33 x 10^{-1} mmol). The resulting solution was refluxed for 50 h until the complete consumption of the starting porphyrin observed by TLC (SiO_2, *n*-hexane/AcOEt = 7:3). Residual NaH was quenched with HCl 1.0 N and CH_2Cl_2 (50.0 mL) was added to the mixture. The organic phase was extracted with H_2O until pH = 7, then dried over Na_2SO_4 and filtered. The solvent was evaporated to dryness under vacuum and the residue purified by flash chromatography (SiO_2, gradient elution from *n*-hexane to *n*-hexane/AcOEt = 7:3) to yield a purple solid **2** (135.0 mg, 60%). ^{1}H NMR (300 MHz, $CDCl_3$): δ 8.90 (s, 4H, $H_{βpyrr}$), 8.84 (d, *J* = 5.4 Hz, 2H, $H_{βpyrr}$), 8.51 (d, *J* = 4.8 Hz, 2H, $H_{βpyrr}$), 8.26 (t, *J* = 6.3 Hz, 6H, H_{Ar}), 7.89 – 7.73 (m, 9H, H_{Ar}), 7.45 - 7.19 (m, 46H, H_{Ar} + $H_{solvent}$), 5.15 (dd, *J* = 13.4, 11.2 Hz, 2H, H_{sugar}), 5.03 – 4.73 (m, 12H, H_{sugar}), 4.73 – 4.60 (m, 2H H_{sugar}), 4.36 (dd, *J* = 17.7, 7.6 Hz, 2H, H_{sugar}), 4.20 (t, *J* = 9.3 Hz, 1H, H_{sugar}), 4.12 (dd, *J* = 11.4, 1.9 Hz, 1H, H_{sugar}), 4.06 – 3.86 (m, 3H, H_{sugar}), 3.85 – 3.74 (m, 3H, H_{sugar}), 3.73 – 3.56 (m, 7H, H_{sugar}), 3.54 - 3.27 (m, 4H, H_{sugar}), -2.73 (s, 2H, NH_{pyrr}). ^{19}F NMR (282 MHz, $CDCl_3$): δ -139.36 (dd, *J* = 24.5, 8.1 Hz, 2F), -156.83 (dd, *J* = 23.7, 8.7 Hz, 2F). ^{13}C NMR (75 MHz, $CDCl_3$): δ 142.38, 142.22, 139.58, 139.05, 138.63, 138.52, 135.01, 134.93, 129.05, 128.98, 128.85, 128.82, 128.78, 128.72, 128.70, 128.65, 128.56, 128.52, 128.48, 128.43, 128.40, 128.37, 128.28, 128.23, 128.19, 128.17, 128.13, 128.08, 128.04, 128.00, 127.95, 127.80, 127.76, 127.70, 127.62, 127.51, 127.16, 127.10, 105.18, 105.08, 102.79, 102.53, 85.23, 84.73, 84.36, 84.10, 83.34, 83.14, 83.07, 82.44, 82.18, 82.11, 81.13, 76.84, 75.43, 75.29, 74.86, 74.38, 73.32, 71.98, 71.51, 57.56, 57.49, 57.44. IR $ν_{max}$ (CH_2Cl_2)/cm^{-1}: 1089, 1200, 1362, 1497, 1453, 1430, 1712, 1989, 3063. UV-Vis: $λ_{max}$ (CH_2Cl_2)/nm (log ε): 418 (4.7), 513 (3.6), 548 (3.2), 588 (3.1), 645 (3.1). LR-MS (ESI): m/z ($C_{99}H_{85}F_4N_4O_{11}$) calcd. 1582.77; found $[M+H]^+$ 1583.6. Elemental analysis calc. for $C_{99}H_{85}F_4N_4O_{11}$ C, 75.13; H, 5.41; N, 3.54; found: C, 75.35; H, 5.70; N, 3.45.

Synthesis of 3. NaH 60% (123.0 mg, 3.08 mmol) was added under nitrogen to a toluene (9.0 mL) solution of **F_{20}TPPH$_2$** (50.0 mg, 5.13 x 10^{-2} mmol) and **1** (368.0 mg, 4.15 x 10^{-1} mmol). The resulting solution was refluxed for 50 h until the complete consumption of the starting porphyrin observed by TLC (SiO_2, *n*-hexane/AcOEt = 7:3). Residual NaH was quenched with HCl 1.0 N and CH_2Cl_2 (15.0 mL) was added to the mixture. The organic phase was extracted with H_2O until pH = 7, then dried over Na_2SO_4 and filtered. The solvent was evaporated to dryness under vacuum and the residue purified by flash chromatography (SiO_2,

gradient elution from *n*-hexane to *n*-hexane/AcOEt = 7:3) to yield a purple solid **3** (95.0 mg, 40%). ^{1}H NMR (400 MHz, $CDCl_3$): δ 8.44 (s, 8H, $H_{βpyrr}$), 7.46 (m, 30H, H_{Ar}), 7.39 – 7.19 (m, 109H, H_{Ar} + $H_{solvent}$), 7.13 (t, *J* = 7.2 Hz, 4H, H_{Ar}), 5.13 (dd, *J* = 16.0, 11.4 Hz, 8H, H_{sugar}), 4.95 – 4.75 (m, 34H, H_{sugar}), 4.66 (dd, *J* = 22.7, 9.9 Hz, 9H, H_{sugar}), 4.52 (d, *J* = 12.1 Hz, 8H, H_{sugar}), 4.36 (d, *J* = 7.6 Hz, 4H, H_{sugar}), 4.20 – 4.11 (m, 8H, H_{sugar}), 4.01 – 3.56 (m, 43H, H_{sugar}), 3.52 – 3.39 (m, 8H, H_{sugar}),- 3.02 (s, 2H, NH_{pyrr}). ^{19}F NMR (376 MHz, $CDCl_3$): δ -138.80 – -138.87 (m, 8F), -156.04 (d, *J* = 17.2 Hz, 8F). ^{13}C NMR (100 MHz, $CDCl_3$): δ 147.74, 145.35, 141.87, 141.70, 139.39, 139.23, 138.70, 138.59, 138.49, 138.19, 138.13, 128.66, 128.57, 128.46, 128.34, 128.31, 128.12, 128.08, 128.03, 127.88, 127.82, 127.78, 127.57, 127.45, 127.42, 127.39, 127.33, 113.88, 113.69, 113.50, 104.84, 104.03, 102.16, 83.80, 83.01, 82.71, 81.78, 80.99, 76.72, 76.46, 75.36, 75.24, 75.02, 74.96, 74.93, 74.52, 73.71, 73.61, 69.49, 68.07, 57.13. IR v_{max} (CH_2Cl_2)/cm^{-1}: 1004, 1060, 1209, 1361, 1399, 1432, 1497, 2626, 2870, 2926, 3061. UV-Vis: $λ_{max}$ (CH_2Cl_2)/nm (log ε): 416 (5.9), 509 (4.2), 538 (4.4), 584 (3.7.), 639 (2.8). LR-MS (MALDI): m/z ($C_{264}H_{248}F_{16}N_4O_{44}$) calcd. 4481.70; found [M] 4481.3. Elemental analysis calc. for ($C_{264}H_{248}F_{16}N_4O_{44}$) C, 70.73; H, 5.53; N, 1.25; found: C, 70.84; H, 5.66; N, 1.24.

Synthesis of 5. Sodium azide (28.0 mg, 4.31 mmol) was added to a DMF (10.0 mL) solution of porphyrin **4** (100.0 mg, 7.71 x 10^{-2} mmol). The resulting solution was stirred at 85 °C for 3 hours until the complete consumption of the porphyrin **4** was observed by TLC (SiO_2, CH_2Cl_2/MeOH = 99:1), then distilled water (30.0 mL) was added and the mixture was extracted with CH_2Cl_2 (3 x 50.0 mL). The organic phase was washed with a saturated solution of NH_4Cl (3 x 50.0 mL), dried over Na_2SO_4 and filtered. The solvent was evaporated to dryness under vacuum and the residue purified by flash chromatography (SiO_2, gradient elution from CH_2Cl_2 to CH_2Cl_2/MeOH = 95:5) to yield a purple solid **5** (150.0 mg, 95%). ^{1}H NMR (400 MHz, $CDCl_3$): δ 8.98 – 8.82 (m, 11H, $H_{βpyrr}$ + H_{Ar}), 8.04 - 7.88 (m, 9H, H_{Ar}), 7.70 – 7.45 (m, 8H, H_{Ar}), 6.76 – 6.18 (m, 16H, H_{Ar}), 3.35 – 3.06 (m, 8H, $H_{CH2\text{-}N3}$), -2.49 (s, 2H, NH_{pyrr}). ^{13}C NMR (100 MHz, $CDCl_3$, 298 K): δ 165.30, 157.39, 138.98, 135.76, 135.63, 135.53, 135.37, 135.08, 130.70, 128.81, 128.56, 126.57, 126.44, 126.16, 126.04, 123.92, 115.54, 53.76, 53.64, 53.55, 53.47. IR v_{max} (CH_2Cl_2)/cm^{-1}: 1091, 1222, 1362, 1428, 1712, 2100, 2962, 3004, 3061, 3407. UV-Vis $λ_{max}$ (CH_2Cl_2)/nm (log ε): 421 (4.7), 483 (3.3), 517 (3.8), 548 (3.4), 592 (3.4), 647 (3.2). LR-MS (ESI): m/z ($C_{76}H_{54}N_{20}O_4$) calcd. 1311.37; found [M+H]$^+$ 1312.4. Elemental analysis calc. for $C_{76}H_{54}N_{20}O_4$: C, 69.61; H, 4.15; N, 21.36; found: C, 69.72; H, 4.15; N, 21.36.

Synthesis of Zn(5). A solution of $Zn(OAc)_2{\cdot}2H_2O$ (375.0 mg, 1.71 mmol) in MeOH (8.0 mL) was added to a CH_2Cl_2 (60.0 mL) solution of **5** (150.0 mg, 1.14 x 10^{-1} mmol). The resulting solution was stirred overnight at room temperature until the complete consumption of **5** was observed by TLC (SiO_2, CH_2Cl_2/MeOH = 99:1), then H_2O (50.0 mL) was added to the mixture. The organic phase was extracted with H_2O (3 x 50.0 mL), dried over Na_2SO_4 and filtered. The solvent was evaporated to dryness under vacuum to give the purple compound Zn(**5**) (155.0 mg, 99%). ^{1}H NMR (400 MHz, $CDCl_3$, 298 K): δ 9.04 – 8.96 (m, 8H, $H_{βpyrr}$), 8.82 - 8.72 (m, 4H, H_{Ar}), 8.11 – 8.09 (m, 1H, H_{Ar}), 8.05 (d, *J* = 7.4 Hz, 1H, H_{Ar}), 8.02 – 7.96 (m, 2H, H_{Ar}), 7.91 – 7.84 (m, 5H, H_{Ar}), 7.68 (s, 1H, H_{NH}), 7.61 – 7.52 (m, 5H, H_{Ar} + H_{NH}), 7.47 (s, 1H, H_{NH}), 7.30 (s, 1H, H_{NH}), 6.75 (d, *J* = 7.5 Hz, 1H, H_{Ar}), 6.62 – 6.57 (m, 3H H_{Ar}), 6.50 – 6.39 (m, 4H, H_{Ar}), 6.38 – 6.29 (m, 4H, H_{Ar}), 6.01 – 5.94 (m, 2H, H_{Ar}), 5.66 – 5.61 (m, 2H, H_{Ar}), 2.97 (s, 1H, $H_{CH2\text{-}N3}$), 2.81 (m, 2H, $H_{CH2\text{-}N3}$), 2.65 (d, *J* = 13.8, 1H, $H_{CH2\text{-}N3}$), 2.55 (m, 3H, $H_{CH2\text{-}N3}$), 2.12 (s, 1H, $H_{CH2\text{-}N3}$). ^{13}C NMR (300 MHz, $CDCl_3$, 298 K): δ 164.75, 152.00, 151.26, 150.78, 138.75, 132.88, 130.28, 123.39, 126.36, 123.58, 121.08, 115.88, 52.82, 52.69, 52.38. IR v_{max} (CH_2Cl_2)/cm^{-1}: 996, 1250, 1308, 1447, 1518, 1581, 1681, 2101, 2340, 2360, 3415. UV-Vis $λ_{max}$ (CH_2Cl_2)/nm (log ε): 425 (5.58), 556 (4.30), 592 (1.20), 626 (2.78) (1.20). LR-MS (ESI): m/z ($C_{76}H_{52}N_{20}O_4Zn$) calcd. 1372.38; found [M+Na]$^+$ 1396.4. Elemental Analysis calc. for $C_{76}H_{54}N_{20}O_4Zn$: C, 66.30; H, 3.95, N, 20.35; found: C, 66, 54; H, 3.99; N, 20.16.

Synthesis of Zn(7). Zn(**5**) (150.0 mg, 1.11 x 10^{-1} mmol) and **6** (276.0 mg, 5.54 x 10^{-1} mmol) were dissolved in THF (20.0 mL) and then a solution of $CuSO_4{\cdot}5H_2O$ (137.0 mg, 5.54 x 10^{-1}mmol) in H_2O (5.0 mL) was added. A solution of sodium ascorbate (109.0 mg, 5.54 x 10^{-1} mmol) in H_2O (5 mL) was added and the resulting mixture was stirred for 5 hours at 50°C until the complete consumption of Zn(**5**) was observed by TLC (SiO_2, CH_2Cl_2/MeOH = 97:3). The mixture was extracted with CH_2Cl_2 (3 x 20.0 mL), dried over Na_2SO_4 and filtered. The solvent was evaporated to dryness under vacuum and the residue purified by flash chromatography (SiO_2, gradient elution from CH_2Cl_2 to CH_2Cl_2/MeOH 98:2) to yield the purple solid **7** (232.0 mg, 63%). ^{1}H NMR (400 MHz, $CDCl_3$, 298 K): δ 8.98 - 8.75 (m, 12 H, $H_{βpyrr}$ + H_{Ar}), 8.09 (t, *J* = 6.6 Hz, 4H, H_{Ar}),7.85 – 7.81 (m, 8H, H_{Ar} + H_{NH}), 7.75 (s, 1H, H_{NH}), 7.61 (s, 1H, H_{NH}), 7.52 – 6.94 (m, 88H, H_{Ar} + $H_{solvent}$), 6.82 – 6.74 (m, 4H, H_{Ar}), 6.66 – 6.47 (m, 12H, H_{Ar}), 6.26 – 6.18 (m, 3H, H_{Ar}), 5.84 – 5.72 (m, 4H, H_{CH2}), 5.52 – 5.48 (m, 2H, H_{CH2}), 5.41 – 5.34 (m, 2H, H_{CH2}), 5.01 – 4.92 (m, 1H, H_{sugar}), 4.84 (d, *J* = 11.2 Hz, 2H, H_{sugar}), 4.72 (q, *J* = 9.5, 7.8 Hz, 6H, H_{sugar}), 4.66 – 4.52 (m, 9H, H_{sugar}), 4.49 – 4.24 (m, 12H, H_{sugar}), 4.22 – 4.14 (m, 2H, H_{sugar}), 4.05 – 3.97 (m, 2H, H_{sugar}), 3.78 (t, *J* = 9.2 Hz, 2H, H_{sugar}), 3.69 – 3.62 (m, 1H, H_{sugar}), 3.57 – 3.39 (m, 8H, H_{sugar}), 3.31 – 3.29 (m, 12H, H_{sugar}), 3.23 – 3.13 (m, 1H, H_{sugar}), 3.04 (d, *J* = 11.6 Hz, 1H, H_{sugar}), 2.93 (t, *J* = 9.4 Hz, 1H, H_{sugar}). ^{13}C NMR (100 MHz, $CDCl_3$, 298 K): δ 139.42, 139.10, 138.41, 128.86, 128.68, 128.50, 128.34, 128.05, 127.89, 119.49, 99.34, 98.47, 82.28, 81,98, 81.42, 80.17, 73.75, 70.67, 70.15, 68.77, 65.58, 65.45, 63.73, 55.99, 52.76. IR v_{max} (CH_2Cl_2)/cm^{-1}: 1047, 1091, 1223, 1273, 1362, 1446, 1519, 1582, 1712, 2928, 3060, 3411. UV $λ_{max}$ (CH_2Cl_2)/nm (log ε): 434 (5.20), 563 (4.08), 602 (3.51). HR-MS (MALDI): m/z ($C_{200}H_{188}N_{20}O_{28}Zn$) calcd. 3383.33, found [M] 3383.6. Elemental Analysis calc. for $C_{200}H_{188}N_{20}O_{28}Zn$: C, 70.96; H, 5.60; N, 8.28; found: C, 71.06; H, 5.70; N, 8.20.

Synthesis of 7. HCl 37% (30.0 mL) was added to a AcOEt (120.0 mL) solution of Zn(**7**) (200.0 mg, 5.92 x 10^{-2} mmol). The resulting solution was stirred for 3 hours at room temperature until the complete consumption of Zn(**7**) was observed by TLC (SiO_2, CH_2Cl_2/MeOH = 97:3), then H_2O (100.0 mL) was added to the mixture. The organic phase was extracted with H_2O (3 x 100.0 mL) until pH = 7. The resulting solution was dried over Na_2SO_4 and filtered. The solvent was evaporated to dryness under vacuum to yield the purple solid **7** (195.0 mg, 99%). ^{1}H NMR (400 MHz, $CDCl_3$, 298 K): δ 8.91 - 8.82 (m, 8H, $H_{βpyrr}$), 8.77 – 8.59 (m, 4H, H_{Ar}), 7.93 – 7.83 (m, 9H, H_{Ar}), 7.72 (s, 2H, H_{triazo}), 7.51 – 7.48 (m, 5H, H_{Ar} + H_{triazo}), 7.31 – 7.07 (m, 63H, H_{Ar} + $H_{solvent}$), 6.89 – 5.86 (m, 19H, H_{Ar}), 4.91 – 4.26 (m, 46H, H_{sugar}), 3.85 – 3.79 (t, *J* = 9.2 Hz, 4H, H_{sugar}), 3.59 –3.49 (m, 20H, H_{sugar}), 3.33 (s, 12H, H_{OMe}), -2.64 (s, 2H, NH_{pyrr}). ^{13}C NMR (100 MHz, $CDCl_3$, 298 K): δ 165.14, 145.69, 145.57, 139.16, 138.73, 138.54, 138.67, 138.45, 138.38, 138.35, 135.89, 135.55, 135.49, 135.35, 135.20, 130.91, 130.67, 130.60, 128.86, 128.78, 128.75, 128.70, 128.64, 128.52, 128.33, 128.25, 128.20, 128.13, 128.07, 127.95, 127.90, 127.85, 127.79, 127.74, 127.33, 126.97, 126.04,125.56, 124.21, 122.85, 122.48, 115.88, 115.62, 98.52, 82.22, 82.18, 80.18, 78.13, 78.07, 75.87, 73.75, 70.24, 68.78, 66.26, 55.60, 52.82. IR v_{max} (CH_2Cl_2)/cm^{-1}: 1047, 1096, 1266, 1306, 1449, 1518, 1582, 1680, 2929, 2960, 3033, 3417. UV-Vis $λ_{max}$ (CH_2Cl_2)/nm (log ε): 424 (5.50), 521 (4.24), 549 (3.70), 591 (3.76), 647 (3.51). HR-MS (MALDI): m/z ($C_{200}H_{190}N_{20}O_{28}$) calcd. 3321.41, found [M+Na]$^+$ 3344.3. Elemental analysis calc. for $C_{200}H_{190}N_{20}O_{28}$: C, 72.32; H, 5.77; N, 8.43; found: C, 72.01; H, 5.88; N, 8.31.

General procedure for the synthesis of iron(III) complexes. $FeBr_2$ (1.42 mmol) was added to a THF (20.0 mL) solution of porphyrin (7.12 x 10^{-2} mmol) under nitrogen. The solution was refluxed at 75°C for 5 hours

until the complete consumption of the starting porphyrin observed by TLC (Al_2O_3, CH_2Cl_2/MeOH = 97:3). The solvent was evaporated to dryness under vacuum and the residue purified by chromatography (Al_2O_3, eluent CH_2Cl_2/MeOH 97:3) to yield a brown solid corresponding to the iron complex. Finally, all the iron complexes were treated at 50°C with MeOH for 8 h. The solvent was evaporated to dryness to afford the desired compound.

Fe(F_5TPP)(OMe) 92% yield. IR ν_{max} (CH_2Cl_2)/cm^{-1}: 1091, 1277, 1273, 1420, 2854, 2927, 3054, 3059. UV-Vis λ_{max} (MeOH)/nm (log ε): 413 (3.7), 478 (2.8), 484 (2.8). LR-MS (ESI): m/z ($C_{45}H_{26}F_5FeN_4O$) calcd. 789.14; found [M-OMe] 759.18. Elemental analysis calc. for $C_{45}H_{26}FeN_4O$: calcd. C, 68.45; H, 3.32; N, 7.10; found C, 68.67; H, 3.63; 6.96.

Fe(2)(OMe) 90% yield. IR ν_{max} (CH_2Cl_2)/cm^{-1}: 1026, 1092, 1271, 1280, 1422, 2927, 2961, 3056. UV-Vis λ_{max} (MeOH)/nm (log ε): 413 nm (5.7), 495 (3.6), 600 (3.4). LR-MS (ESI) m/z: ($C_{100}H_{85}F_4FeN_4O_{12}$) calcd. 1665.54, found $[M+Na]^+$ 1688.59. Elemental analysis calc. for $C_{100}H_{85}F_4FeN_4O_{12}$ C 72.07, H 5.14, N 3.36; found: C, 72.25; H, 5.35; N, 3.30.

Fe(3)(OMe) 95% yield. IR ν_{max} (CH_2Cl_2)/cm^{-1}: 1081, 1259, 1266, 1278, 2857, 2926, 3058. UV-Vis λ_{max} (MeOH)/nm (log ε): 410 (5.1), 519 (3.8), 580 (3.7). HR-MS (MALDI): m/z ($C_{265}H_{249}F_{16}FeN_4O_{45}$) calcd. 4566.64, found $[M\text{-}OMe+Na]^+$ 4559.2. Elemental analysis calc. for $C_{265}H_{249}F_{16}FeN_4O_{45}$ C, 69.65; H, 5.49; N, 1.23; found: C, 69.83; H, 5.62, N, 1.21.

Fe(7)(OMe) 92% yield. IR ν_{max} (CH_2Cl_2)/cm^{-1}: 1447, 1452, 1512, 1582, 1680, 2867, 2928, 2960, 3417. UV-Vis λ_{max} (CH_2Cl_2)/nm (log ε) 421 (5.43), 478 (4.78), 581 (4.39). HR-MS (MALDI): m/z ($C_{201}H_{191}FeN_{20}O_{28}$) calcd. 3406.35, found [M-OMe] 3375.0. Elemental analysis calc. for $C_{201}H_{191}FeN_{20}O_{28}$: C 70.87, H 5.65, N 8.22; found C 70.97, H 5.75, N 8.15.

Synthesis of Ru(F_5TPP)(CO) and Ru(2)(CO). Ru_3CO_{12} (2.13 x 10^{-1} mmol) was added to a 1,2,4-trichlorobenzene (20.0 mL) solution of porphyrin (7.12 x 10^{-2} mmol) under nitrogen. The solution was refluxed for 5 hours until the complete consumption of the starting porphyrin was observed by TLC (SiO_2, *n*-hexane/AcOEt = 7:3). The solvent was evaporated to dryness under vacuum and the residue purified by chromatography (SiO_2, gradient elution from *n*-hexane to *n*-hexane/AcOEt = 7:3) to yield a red solid corresponding to the ruthenium complex.

Ru(F_5TPP)(CO) 68% yield**.** ^{1}H NMR (300 MHz, $CDCl_3$): δ 8.78 (d, *J* = 4.9 Hz, 2H, $H_{\beta pyrr}$), 8.69 (s, 4H, $H_{\beta pyrr}$), 8.61 (d, *J* = 4.9 Hz, 2H, $H_{\beta pyrr}$), 8.25 – 8.09 (m, 6H, H_{Ar}), 7.82 – 7.67 (m, 9H, H_{Ar}). ^{19}F NMR (282 MHz, $CDCl_3$): δ -136.62 (dd, *J* = 24.2, 9.0 Hz, 1F), -138.24 (d, *J* = 24.3 Hz, 1F), -153.73 (t, *J* = 21.0 Hz, 1F), -162.48 (t, *J* = 23.4 Hz, 1F), -163.06 (d, *J* = 23.9 Hz, 1F). ^{13}C NMR (75 MHz, $CDCl_3$): δ 144.59, 144.18, 144.15, 143.16, 142.09, 142.03, 138.76, 134.41, 133.81, 133.37, 132.24, 131.90, 129.48, 128.04, 127.56, 126.97, 126.70, 126.64, 126.49, 123.97, 123.54, 122.53. IR ν_{max} (CH_2Cl_2)/cm^{-1}: 1010, 1094, 1273, 1282, 1494, 1520, 1942, 2962, 3004, 3056, 3063, 3415. UV-Vis λ_{max} (CH_2Cl_2)/nm (log ε): 408 (3.9), 528 (2.9), 553 (2.7). LR-MS (ESI): m/z ($C_{45}H_{23}F_5N_4ORu$) calcd. 832.08 found [M-CO] 804.04. Elemental analysis calc. for $C_{45}H_{23}F_5N_4ORu$ C, 64.98; H, 2.79; C, 6.74; found C, 65.25; H, 3.09; N, 6.62.

Ru(2)(CO) 61% yield. ^{1}H NMR (300 MHz, $CDCl_3$): δ 8.71 – 8.36 (m, 8H, $H_{\beta pyrr}$), 8.34 – 8.12 (m, 9H, H_{Ar}), 7.80 – 7.58 (m, 16H, H_{Ar}), 7.40 – 7.26 (m, 77H, H_{Ar} + $H_{solvent}$), 5.16 – 3.67 (br, 29H, H_{sugar}). ^{19}F NMR (282 MHz, $CDCl_3$): δ -137.94 – -140.21 (m, 2F), -156.17 – -157.34 (m, 2F). ^{13}C NMR (75 MHz, $CDCl_3$): δ 135.01, 134.93, 129.05, 128.98, 128.85, 128.82, 128.78, 128.72, 128.70, 128.65, 128.56, 128.52, 128.48, 128.43, 128.40, 128.37, 128.28, 128.23, 128.19, 128.17, 128.13, 128.08, 128.04, 128.00, 127.95, 127.80, 127.76, 127.70, 127.62, 127.51, 127.16, 127.10, 105.18, 105.08, 102.79, 102.53, 85.23, 84.73, 84.36, 84.10, 83.34, 83.14, 83.07, 82.44, 82.18, 82.11, 81.13, 75.43, 75.29, 74.86, 74.38, 73.32, 71.98, 71.51, 57.56, 57.49, 57.44. IR ν_{max} (CH_2Cl_2)/cm^{-1}: 1009, 1095, 1262, 1275, 1282, 1941, 2926, 2960, 2986, 3051, 3060. UV-Vis λ_{max} (CH_2Cl_2)/nm (log ε): 406 (5.1), 527 (3.8), 550 (3.6). LR-MS (ESI) m/z ($C_{100}H_{82}F_4N_4O_{12}Ru$) calcd. 1708.40, found $[M+K]^+$ 1746.7. Elemental analysis calc. for $C_{100}H_{82}F_4N_4O_{12}Ru$ C, 70.29; H, 4.84; N, 3.28; found: C, 70.49; H, 5.05; N, 3.22.

Synthesis of Ru(3)(CO). NaH 60% wt (166.4 mg, 4.16 mmol) was added under nitrogen to a toluene (14.0 mL) solution of Ru(**F_{20}TPP**)(CO) (115.0 mg, 0.104 mmol) and **1** (290.0 mg, 0.624 mmol). The solution was refluxed for 50 hours until the complete consumption of Ru(**F_{20}TPP**)(CO) was observed by TLC (SiO_2, *n*-hexane/AcOEt = 7:3) and then residual NaH was quenched with HCl 1.0 N. CH_2Cl_2 (20.0 mL) was added to the mixture, the organic phase was extracted with H_2O until pH = 7, dried over Na_2SO_4 and filtered. The solvent was evaporated to dryness under vacuum and the resulting residue was purified by flash chromatography (SiO_2, gradient elution from *n*-hexane to *n*-hexane/AcOEt = 6:4) to yield the red solid Ru(**3**)(CO) (197.0 mg, 39%). ^{1}H NMR (400 MHz, $CDCl_3$): δ 8.30 - 8.24 (m, 8H,$H_{\beta pyrr}$), 7.44 – 7.23 (m, 187H, H_{Ar} + $H_{solvent}$), 5.10 (t, *J* = 11.9 Hz, 9H, H_{sugar}), 4.92 – 4.73 (m, 40H, H_{sugar}), 4.64 (dd, *J* = 20.9, 9.4 Hz, 14H, H_{sugar}), 4.50 (d, *J* = 11.6 Hz, 10H, H_{sugar}), 4.34 (d, *J* = 7.5 Hz, 6H, H_{sugar}), 4.17 – 4.08 (m, 9H, H_{sugar}), 3.96 – 3.87 (m, 10H, H_{sugar}), 3.78 – 3.60 (m, 15H, H_{sugar}), 3.58 – 3.48 (m, 25H, H_{sugar}), 3.46 – 3.39 (m, 12H, H_{sugar}). ^{19}F NMR (376 MHz, $CDCl_3$): δ -138.18 – -140.32 (m, 8F), -155.84 – -156.90 (m, 8F). ^{13}C NMR (100 MHz, $CDCl_3$) δ 144.00, 139.21, 138.68, 138.49, 138.25, 138.16, 128.65, 128.59, 128.43, 128.30, 128.12, 128.07, 128.01, 127.79, 127.75, 127.56, 127.39, 127.31, 104.81, 102.12, 83.73, 83.00, 82.67, 81.76, 80.94, 76.43, 75.31, 75.20, 75.00, 74.97, 74.90, 74.55, 73.64, 73.58, 69.46, 68.05, 57.11. IR ν_{max} (CH_2Cl_2)/cm^{-1}: 1080, 1270, 1360, 1420, 1497, 1954, 2871, 2987, 3052. UV-Vis λ_{max} (CH_2Cl_2)/nm (log ε): 408 (5.1), 528 (3.9), 550 (3.7). MS (MALDI) m/z: ($C_{265}H_{246}F_{16}N_4O_{45}Ru$) calcd. 4609.59, found [M-CO] 4581.8. Elemental analysis calc. for $C_{265}H_{246}F_{16}N_4O_{45}Ru$: C, 69.01; H, 5.38; N, 1.21, found C, 69.30; H, 5.56, N, 1.19.

Synthesis of Ru(7)(CO). Ru_3CO_{12} (2.13 x 10^{-1} mmol) was added to a toluene (15.0 mL) solution of **7** (7.12 x 10^{-2} mmol) under nitrogen. The solution was refluxed in pressure tube for 8 hours until the complete consumption of **7** was observed by TLC (SiO_2, CH_2Cl_2/*n*-hexane = 1:1). The solvent was evaporated to dryness under vacuum and the resulting residue was purified by flash chromatography (SiO_2, gradient elution from *n*-hexane/AcOEt = 7:3 to *n*-hexane/AcOEt = 1:1) to yield the brown solid Ru(**7**)(CO) (197.0 mg, 19%). ^{1}H and ^{13}C NMR spectra (400 MHz, $CDCl_3$) were not well-resolved. IR ν_{max} (CH_2Cl_2)/cm^{-1}: 1094, 1420, 1520, 1582, 1680, 1681, 1948, 2023, 2305, 2855, 2958, 3054. UV-Vis λ_{max} (CH_2Cl_2)/nm (log ε): 417 (5.1), 535 (4.1), 598 (3.7). HR-MS (MALDI) m/z: ($C_{201}H_{189}N_{20}O_{29}Ru$) calcd. 3448.30, found [M-CO] 3418.2 Elemental Analysis calc. for $C_{201}H_{189}N_{20}O_{29}Ru$ C, 70.00; H, 5.49; N, 8.12; found: C, 70.29; H, 5.70; N, 7.96.

General procedure for cyclopropanation reactions. *Method A*: In a typical run, the catalyst (6.79 x 10^{-4} mmol) was dissolved in 2.0 mL of dry toluene before adding the alkene (3.39 mmol) and the diazo compound (7.47 x 10^{-1} mmol) under nitrogen. The reaction was stirred for 2 hours at 25°C. The solution was then evaporated to dryness and the reaction crude was analysed by ^{1}H-NMR spectroscopy using 2,4-dinitrotoluene as the internal standard. *Method B:* the procedure illustrated for method A was followed using 6.79 x 10^{-1} mmol of alkene.

General procedure for aziridination reactions. In a typical run, the catalyst (2.72 x 10^{-2} mmol) was dissolved in 6.0 mL of dry benzene before adding the azide (1.34 x 10^{-1} mmol) and the alkene (6.79 x 10^{-1} mmol) under nitrogen. The resulting solution was refluxed using a preheated oil bath for two 2 hours. The solution was then evaporated to dryness and the reaction crude was analysed by ^{1}H-NMR spectroscopy using 2,4-dinitrotoluene as the internal standard.

Keywords: glycoporphyrin • iron • ruthenium • aziridination • cyclopropanation

[1] a) G. Kumari, Nutan, M. Modi, S. K. Gupta, R. K. Singh, *Eur. J. Med. Chem.* **2011**, *46*, 1181-1188; b) A. Nikitjuka, A. Jirgensons, *Chem. Heterocycl. Compd.* **2014**, *49*, 1544-1559.

[2] a) M. P. Doyle, R. Duffy, M. Ratnikov, L. Zhou, *Chem. Rev.* **2010**, *110*, 704-724; b) D. Intrieri, P. Zardi, A. Caselli, E. Gallo, *Chem. Commun.* **2014**, *50*, 11440-11453.

[3] a) N. Jung, S. Bräse, *Angew. Chem. Int. Ed.* **2012**, *51*, 5538-5540; b) A. Roy, S. P. Goswami, A. Sarkar, *Synth. Commun.* **2018**, *48*, 2003-2036.

[4] a) D. Intrieri, D.M. Carminati, E. Gallo in *Recent Advances in Metal Porphyrinoid-Catalyzed Nitrene and Carbene Transfer Reactions* (Eds.: K.M.S. Kadish, M. Kevin, Roger Guilard), Handbook of Porphyrin Science, World Scientific Publishing Co. Pte. Ltd. **2016**, pp. 1-99; b) C. Damiano, D. Intrieri, E. Gallo, *Inorg. Chim. Acta* **2018**, *470*, 51-67; c) B. J. Anding, L. K. Woo in *An overview of Metalloporphyrin-catalyzed Carbon and Nitrogen Group Transfer Reactions* (Eds.: K.M.S. Kadish, M. Kevin, Roger Guilard), Handbook of Porphyrin Science, World Scientific Publishing Co. Pte. Ltd. **2012**, pp. 145-319; d) C. Ebner, E. M. Carreira, *Chem. Rev.* **2017**, *117*, 11651-11679; e) G. T. Gurmessa, G. S. Singh, *Res. Chem. Intermed.* **2017**, *43*, 6447-6504.

[5] a) D. V. Titov, M. L. Gening, Y. E. Tsvetkov, N. E. Nifantiev, *Russ. Chem. Rev.* **2014**, *83*, 523-554; b) M. Ethirajan, Y. Chen, P. Joshi, R. K. Pandey, *Chem. Soc. Rev.* **2011**, *40*, 340-362; c) G. Garcia, F. Hammerer, F. Poyer, S. Achelle, M.-P. Teulade-Fichou, P. Maillard, *Bioorg. Med. Chem.* **2013**, *21*, 153-165; d) S. Singh, A. Aggarwal, N. V. S. D. K. Bhupathiraju, G. Arianna, K. Tiwari, C. M. Drain, *Chem. Rev.* **2015**, *115*, 10261-10306.

[6] a) C.-M. Ho, J.-L. Zhang, C.-Y. Zhou, O.-Y. Chan, J. J. Yan, F.-Y. Zhang, J.-S. Huang, C.-M. Che, *J. Am. Chem. Soc.* **2010**, *132*, 1886-1894; b) S. Vilain-Deshayes, A. Robert, P. Maillard, B. Meunier, M. Momenteau, *J. Mol. Catal. A: Chem.* **1996**, *113*, 23-34.

[7] G. Tseberlidis, P. Zardi, A. Caselli, D. Cancogni, M. Fusari, L. Lay, E. Gallo, *Organometallics* **2015**, *34*, 3774-3781.

[8] I. D. Mackie, J. Röhrling, R. O. Gould, J. Pauli, C. Jäger, M. Walkinshaw, A. Potthast, T. Rosenau, P. Kosma, *Carbohydr. Res.* **2002**, *337*, 161-166.

[9] B. L. Auras, S. De Lucca Meller, M. P. da Silva, A. Neves, L. H. Z. Cocca, L. De Boni, C. H. da Silveira, B. A. Iglesias, *Appl. Organomet. Chem.* **2018**, *32*, e4318.

[10] J. S. Lindsey, R. W. Wagner, *J. Org. Chem.* **1989**, *54*, 828-836.

[11] A. Didier, L. Michaudet, D. Ricard, V. Baveux-Chambenoît, P. Richard, B. Boitrel, *Eur. J. Org. Chem.* **2001**, 1917-1926.

[12] H. B. Mereyala, S. R. Gurrala, S. K. Mohan, *Tetrahedron* **1999**, *55*, 11331-11342.

[13] J. P. Collman, R. R. Gagne, C. Reed, T. R. Halbert, G. Lang, W. T. Robinson, *J. Am. Chem. Soc.* **1975**, *97*, 1427-1439.

[14] a) D. Intrieri, S. Le Gac, A. Caselli, E. Rose, B. Boitrel, E. Gallo, *Chem. Commun.* **2014**, *50*, 1811-1813; b) D. M. Carminati, D. Intrieri, A. Caselli, S. Le Gac, B. Boitrel, L. Toma, L. Legnani, E. Gallo, *Chem. Eur. J.* **2016**, *22*, 13599-13612; c) D. M. Carminati, D. Intrieri, Stéphane Le Gac, T. Roisnel, B. Boitrel, L. Toma, L. Legnani, E. Gallo, *New J. Chem.*, **2017**, *41*, 5950-5959.

[15] Y. Liu, C.-M. Che, *Chem.-Eur. J.* **2010**, *16*, 10494-10501.

[16] S. Fantauzzi, E. Gallo, A. Caselli, C. Piangiolino, F. Ragaini, S. Cenini, *Eur. J. Org. Chem*. **2007**, 6053-6059.

[17] a) S. Bräse, K. Banert, Editors, *Organic Azides Syntheses and Applications*, John Wiley & Sons Ltd., **2010**; b) S. Kumar, A. S. Pathania, N. K. Satti, P. Dutt, N. Sharma, F. A. Mallik, A. Ali, *Eur. J. Med. Chem.* **2015**, *92*, 236-245.

[18] a) Y. Zhang, J. Li, X. Yang, P. Zhang, J. Pang, B. Li, H.-C. Zhou, *Chem. Commun.* **2019**, *55*, 2023-2026; b) H. M. L. Davies, T. Hansen, M. R. Churchill, *J. Am. Chem. Soc.* **2000**, *122*, 3063-3070.

[19] C.-M. Che, J.-L. Zhang, R. Zhang, J.-S. Huang, T.-S. Lai, W.-M. Tsui, X.-G. Zhou, Z.-Y. Zhou, N. Zhu, C. K. Chang, *Chem. Eur. J.* **2005**, *11*, 7040-7053.

Entry for the Table of Contents

FULL PAPER

The one-pot synthesis of cyclopropanes and aziridines was efficiently promoted by glycoporphyrin-based catalysts. The catalytic effect of the number and location of carbohydrate units on the porphyrin skeleton was investigated.

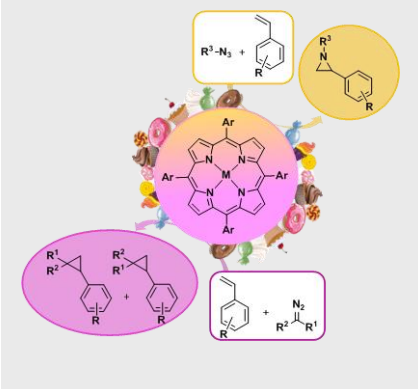

Glycoporphyrin Complexes

Caterina Damiano, Sebastiano Gadolini, Daniela Intrieri, Luigi Lay, Cinzia Colombo and Emma Gallo**

Page No. – Page No.

Iron and Ruthenium Glycoporphyrins: Active Catalysts for the Synthesis of Cyclopropanes and Aziridines